Journal of Microbiology (2024) 62:627–637
https://doi.org/10.1007/s12275-024-00143-y

MICROBIAL GENETICS, GENOMICS AND MOLECULAR BIOLOGY

RapB Regulates Cell Adhesion and Migration in *Dictyostelium,* Similar to RapA

Uri Han[1] · Nara Han[1] · Byeonggyu Park[1] · Taeck Joong Jeon[1,2]

Received: 12 March 2024 / Revised: 22 April 2024 / Accepted: 3 May 2024 / Published online: 17 June 2024

Abstract

Ras small GTPases act as molecular switches in various cellular signaling pathways, including cell migration, proliferation, and differentiation. Three Rap proteins are present in *Dictyostelium*; RapA, RapB, and RapC. RapA and RapC have been reported to have opposing functions in the control of cell adhesion and migration. Here, we investigated the role of RapB, a member of the Ras GTPase subfamily in *Dictyostelium*, focusing on its involvement in cell adhesion, migration, and developmental processes. This study revealed that RapB, similar to RapA, played a crucial role in regulating cell morphology, adhesion, and migration. *rapB* null cells, which were generated by CRISPR/Cas9 gene editing, displayed altered cell size, reduced cell-substrate adhesion, and increased migration speed during chemotaxis. These phenotypes of *rapB* null cells were restored by the expression of RapB and RapA, but not RapC. Consistent with these results, RapB, similar to RapA, failed to rescue the phenotypes of *rapC* null cells, spread morphology, increased cell adhesion, and decreased migration speed during chemotaxis. Multicellular development of *rapB* null cells remained unaffected. These results suggest that RapB is involved in controlling cell morphology and cell adhesion. Importantly, RapB appears to play an inhibitory role in regulating the migration speed during chemotaxis, possibly by controlling cell-substrate adhesion, resembling the functions of RapA. These findings contribute to the understanding of the functional relationships among Ras subfamily proteins.

Keywords Ras proteins · RapB · RapA · RapC · Cell migration · *Dictyostelium*

Introduction

Ras proteins are small monomeric GTPases that act as molecular switches in the signal transduction of diverse cellular processes, including directional cell migration upon external stimuli (Artemenko et al., 2014; Kortholt & van Haastert, 2008; Wennerberg et al., 2005). Successful chemotaxis, the process by which cells move toward chemoattractants, requires the polarization of cells in response to these stimuli, leading to the formation of the anterior and posterior regions of migrating cells. Cell surface G-protein-coupled receptors (GPCRs) detect shallow gradients of external chemoattractants (Artemenko et al., 2014; Kölsch et al., 2008). Ras proteins play a critical role in amplifying these shallow gradients of external chemoattractants into polarized internal signaling molecules, such as including phosphatidylinositol 3-kinases (PI3Ks) and F-actin-related proteins, which are differentially localized at the front and back of the cells (Artemenko et al., 2014; Kölsch et al., 2008; Sasaki et al., 2007). Ras proteins are rapidly and transiently activated in response to chemoattractant stimulation. Activated Ras proteins are enriched at the leading edge of chemotaxing cells, where they locally activate signaling molecules, including PI3Ks. The asymmetrical activation of Ras proteins at the leading edge helps guide the local polymerization of F-actin and pseudopod extension at the front and actomyosin-driven contraction at the lateral and posterior regions of migrating cells (Artemenko et al., 2014; Kölsch et al., 2008; Kortholt & van Haastert, 2008; Lee & Jeon, 2012).

The *Dictyostelium* Ras GTPase subfamily contains 15 proteins, consisting of 11 Ras, 3 Rap and 1 Rheb-related protein. Among these, RapA (also known as Rap1), RapB, and

✉ Taeck Joong Jeon
tjeon@chosun.ac.kr

[1] Department of Integrative Biological Sciences and BK21 FOUR Educational Research Group for Age-Associated Disorder Control Technology, Chosun University, Gwangju 61452, Republic of Korea

[2] The Basic Science Institute of Chosun University, Chosun University, Gwangju 61452, Republic of Korea

RapC constitute the *Dictyostelium* Rap proteins (Kortholt & van Haastert, 2008; Lee & Jeon, 2012). RapA serves as a key regulator of integrin-mediated cell adhesion and cadherin-mediated cell–cell adhesion (Bos, 2018; Kortholt & van Haastert, 2008). RapA is rapidly activated in the anterior region of migrating cells in response to cAMP chemoattractants. Activated RapA regulates the establishment of cell polarity by locally modulating myosin II disassembly in the anterior region of cells via the RapA/Phg2 signaling pathway. Myosin II disassembly at the leading edge of migrating cells, mediated by RapA/Phg2, facilitates F-actin polymerization (Jeon et al., 2007b; Lee & Jeon, 2012). Subsequently, the assembled F-actin at the leading edge recruits RapA deactivating proteins, such as RapGAP1, to the cell cortex at the front of the cell, leading to RapA deactivation (Jeon et al., 2007a; Lee & Jeon, 2012). This deactivation primes RapA for a new cycle of cytoskeletal reorganization and cell attachment. RapA has also been linked to the control of F-actin polymerization via its interaction with RacGEF1 (Lee & Jeon, 2012; Mun & Jeon, 2012).

Recently, RapC has emerged as a regulator of cell adhesion and multicellular development (Park et al., 2018). However, their functions appear to differ from those of RapA. RapC-deficient cells exhibit a spread morphology and reduced migration speed, possibly due to increased cell adhesion, suggesting that RapC plays a negative role in cell spreading and adhesion. RapC has a unique function during multicellular developmental processes, particularly in tip formation from mounds (Jeon et al., 2021; Park et al., 2018). Notably, the C-terminus of RapC, which is absent from RapA, is crucial for these opposing functions and reverse the functions of RapA when fused to the tail (Kim et al., 2021).

Three Rap proteins exist in *Dictyostelium*: RapA, RapB, and RapC. However, unlike RapA and RapC, RapB's role in cell adhesion and migration remains uncharacterized. To investigate the functions of RapB in cell migration and development, we generated *rapB* null cells using CRISPR/Cas9 system and assessed the phenotypes of these cells. In addition, we explored the relationship between RapA, RapB, and RapC by examining the phenotypes of *rapB* null cells expressing either RapA or RapC.

Materials and Methods

Cell Strains and Cell Culture

Dictyostelium discoideum wild-type Ax2 (DBS0237914) and KAx3 cells (DBS0236487) were obtained from the *Dictyostelium* Stock Center, and were cultured axenically in HL5 medium at 22 °C. *rapB* gene-edited cells from the parental strain Ax2 were generated by CRISPR/Cas9 gene editing system (Muramoto et al., 2019; Sekine et al., 2018). The full coding sequences of *rapB* and *rapC* cDNAs were generated by RT-PCR with gene-specific primers and cloned into the *Eco*RI – *Xho*I site of the expression vector pEXP-4(+) containing a GFP fragment, respectively. The expression plasmids were confirmed by sequencing and transformed into wild-type Ax2 or KAx3 cells. Transformants were maintained in 20 μg/ml G418 or 10 μg/ml blasticidin, as appropriate.

CRISPR/Cas9 Gene Editing

rapB gene edited cells were generated by CRISPR/Cas9 gene editing system using the all-in-one sgRNA and Cas9 expression vector, pTM1285 as described previously (Sekine et al., 2018). The CRISPR target site containing the NGG PAM sequence in *rapB* gene was identified using E-CRISP design. A pair of oligonucleotides corresponding to the CRISPR target site were synthesized with overhang sequences AGCA and AAAC, respectively: RapB-edit-forward (AGCAGTAATGGGGCGCTGGTTCAGT) and RapB-edit-reverse (AAACACTGAACCAGCGCCCATTAC). The annealed oligonucleotides were cloned into the pTM1285 vector using Golden Gate cloning method (New England BioLabs), producing pTM1285-RapB. The insertion of *rapB* sgRNA into the pTM1285 vector were examined by PCRs with a pair of primers; RapB-edit-forward and Tracr-reverse (AAGCTTAAAAAAAGCACCGACTCGGTGCC) which are located within the vector for sequencing and the PCR product is 123 bp.

The pTM1285-RapB plasmids were transformed into Ax2 wild-type cells by electroporation. The transformed cells were cultured in HL5 for 24 h and then maintained for another 2 days or 7 days in the presence of 10 μg/ml G418. After treating the cells with G418, the cells were plated on SM agar plates with bacteria (*Klebsiella aerogenes*) and incubated until plaques were formed. To sequence the target regions edited by CRISPR/Cas9 system in individual clones, genomic DNAs from each clone were isolated and used in PCRs with the following RapB-specific primers: RapB-I-F (CCCGAATTCATCAAAAGATTCAAAAGG) and RapB-II-R (CCCGGATCCGTACACTAATATAAAACC) (Fig. S1). Two primers (I/II) are located to include the gene-edited region in the PCR products. The amplified PCR products were sequenced using a RapB-II-R primer. To confirm the gene-edited mutants, total RNAs from wild-type and the selected clone cells were extracted and used in RT-PCRs using two primers (I/II) or (I/III). Primer III (AGCCGGGAAACTCCTAGTGG) is specific to the inserted region of a 144-bp insertion mutant.

Site-Directed Mutagenesis

The mutants GFP-RapB^{G31V} and GFP-RapB^{S36N} were generated using pGFP-RapB and the Quik-Change Site-Directed Mutagenesis kit (Stratagene) (Jeon et al., 2007b). To determine which amino acids are critical for RapB function, *D. discoideum* RapB (dRapB) were compared with other Ras proteins using multiple sequence alignments (Fig. S1). As dRapB contains 19 additional N-terminal amino acids compared with the human Ras proteins and *Dictyostelium* RasG (dRasG), glycine at amino acid 31 and serine at amino acid 36 in dRapB correspond to glycine at amino acid 12 and serine at amino acid 17 in other Ras proteins, respectively. It has been reported that point-mutation of glycine at position 12 to valine (G12V) or serine at position 17 to asparagine (S17N) make the Ras proteins the constitutively activated or the dominantly negative form, respectively (Jeon et al., 2007b; Rebstein et al., 1997). For the constitutively activated form of RapB, glycine at amino acid 31 in dRapB was replaced with valine using two primers; RapB-CA-F (GCAGTAATGGGCGCTGTTTCAGTTGGTAAATCAGC) and RapB-CA-R (GCTGATTTACCAACTGAAACAGCG CCCATTACTGC). For the dominantly negative form of RapB, serine at amino acid 36 was replaced with asparagine with two primers; RapB-DN-F (CAGTTGGTAAAA ATGCACTCACTGTTCAATTCACTC) and RapB-DN-R (GAGTGAATTGAACAGTGAGTGCATTTTTACCAA CTG). The mutant plasmids were transformed into KAx3 wild-type cells.

Cell Adhesion

Cell adhesion assay was performed as described previously (Mun et al., 2014). Mid Log-phase growing cells on the plates were washed and resuspended at a density of 3.5×10^7 cells/ml in 12 mM Na/K phosphate buffer. 150 µl of the cells were placed and attached on the 6-well culture dishes. Before shaking the plates, the cells were photographed and counted to calculate the total cell number. To detach the cells from the plates, the plates were shaken at 150 rpm for 30 min, and then the attached cells were photographed and counted for the attached cell number after the medium containing detached cells was removed. Cell adhesion was presented as a percentage of attached cells compared with total cells.

Chemotaxis

Chemotaxis towards cAMP was examined as described previously (Lee & Jeon, 2012; Mun et al., 2014). The aggregation-competent cells were prepared by pulsing with 7.5 µM cAMP at the density of 5×10^6 cells/ml in Na/K phosphate buffer for 6 h. Cell migration was analyzed using a Under Agarose Assay chamber. The images of chemotaxing cells were taken at time-lapse intervals of 1 min for 1 h using an inverted microscope (IX71; Olympus). The data were analyzed using the NIS-Elements software (Nikon) and Image J software (National Institutes of Health, NIH). Trajectory speed was used to quantify motility of the cells. The trajectory speed is the total distance moved of a cell every 1 min in a time-lapse recording. Directionality is measure of how straight the cells move. Cells moving in a straight line have a directionality of 1. It was calculated as the distance moved over the linear distance between the start and the finish.

Multicellular Development

Development assay was performed as described previously (Jeon et al., 2009). Exponentially growing cells were harvested and washed twice with 12 mM Na/K phosphate buffer (pH 6.1) and resuspended at a density of 3.5×10^7 cells/ml. 50 µl of the cells were placed on Na/K phosphate agar plates and developed for 24 h. The developmental morphologies of the cells were photographed and examined under a phase-contrast microscope.

RT-PCR

The total RNAs from wild-type and *rapB* null cells were extracted by using the SV Total RNA Isolation system (Promega), and the cDNAs were synthesized by reverse transcription with MMLV reverse transcriptase (Promega) using random hexamer and 0.5 µg of total RNAs. 1 µl of the cDNAs were used in following PCR with 35 cycles employing gene-specific primers. The universal 18S ribosomal RNA specific primers were used as an internal control (Jeon et al., 2007a); 18S rRNA-F (GTAATTCCAGCTCCA ATAGC) and 18S rRNA-R (GAACGGCCATGCACCAC).

Statistical Analysis

Statistical analysis was performed using Student's t-test (two-tailed). All data was collected from at least three independent experiments and expressed as the means ± standard deviation (SD). P value less than 0.05 was considered as statistically significant.

Results

Domain Structure of RapB and CRIPR/Cas9-Mediated RapB Mutants

Dictyostelium contains 15 Ras subfamily proteins, three of which are Rap proteins: RapA, RapB, and RapC. RapA is a key regulator of cytoskeletal assembly/disassembly that

controls cell migration and adhesion (Kortholt & van Haastert, 2008). A recent study has shown that RapA and RapC play opposite roles in controlling cell adhesion and migration, although they play some specific roles in cytokinesis and development (Jeon et al., 2021). Unlike RapA and RapC, RapB has not yet been characterized.

RapB (DDB_G0272857) is composed of 205 amino acids and contains a RAS domain in the middle of the protein (Fig. 1). In contrast to RapA and RapC, a stretch of 19 amino acids was found in the N-terminal region of RapB and its estimated molecular mass is 23 kDa. Multiple alignments of the Ras domain of RapB with those of other Ras proteins showed 53.6% and 38.1% identities with those of RapA and RapC, respectively. RapB contains a highly conserved catalytic domain, a set of conserved G-box GDP/GTP-binding motifs, effector-binding domains, and a C-terminal hypervariable region (Bos, 2018; Wennerberg et al., 2005; Zhou & Hancock, 2015) (Fig. S1). Most Ras family proteins terminate with a C-terminal CAAX (C = Cys, A = aliphatic, X = any amino acid) tetrapeptide sequence, which is a recognition sequence for prenylation. RapB and RapC have a farnesylation site at the C terminus (if X = Ser, Ala, Met, Cys, and Gln), whereas RapA has a geranylgeranylation signal (if X = Leu or Glu) (Simanshu et al., 2017; Zhou & Hancock, 2015).

To investigate the function of RapB, we prepared *rapB*-edited mutants using the CRISPR/Cas9 gene-editing system (Muramoto et al., 2019; Sekine et al., 2018), and the strains were confirmed via gene sequencing and RT-RCR (Fig. 1C and Fig. S1). We obtained seven clones, grouped into four gene-edited mutants (Fig. 1). Each of the two clones had a 5-bp deletion, a 5-bp insertion, and a 3-bp insertion. One clone had a 144-bp insertion, which was identified to the partial sequence of *E. coli* (CP139677.1). The 144-bp insertion mutant was used in further studies as *rapB* null cells since the insertion was confirmed by both PCRs using gDNAs and RT-PCRs. PCRs using gDNAs with gene-specific primers I/II produced a band of 553 bp in wild-type cells and a band of 697 bp in the 144-bp insertion mutants (Fig. S1B, left panel). Reverse transcription (RT)-PCR using primer set I/

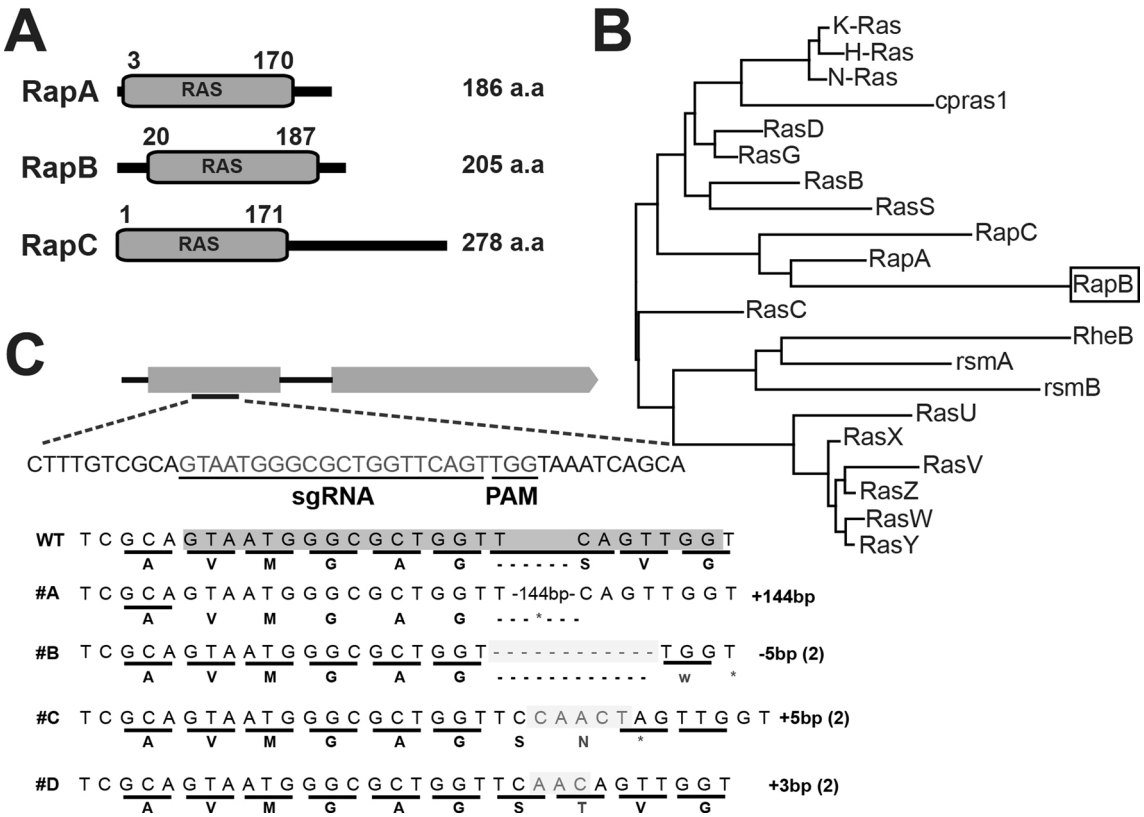

Fig. 1 Domain structure and phylogenetic tree of Ras subfamily proteins. **A** Domain structure of RapA, RapB, and RapC containing a Ras domain. **B** Phylogenetic tree of Ras subfamily proteins. Rap proteins are grouped and RapB is the closest to RapA. RapB was boxed. The amino acid sequences of Ras proteins are available at DictyBase site. **C** CRISPR/Cas9-mediated *rapB* mutants. Schematic view of sgRNA and PAM motif targeting locus of the *rapB* gene are presented. The underlined sequence indicates the target site of the sgRNA. The PAM sequence was marked. *rapB* edited mutants from two independent experiments were grouped into four; 1 clone with a 144-bp insertion, 2 clones with a 5-bp deletion, 2 clones with a 5-bp insertion, and 2 clones with a 3-bp insertion. The changed amino acids and a stop codon were marked. Numbers in parentheses indicate the number of identical clones

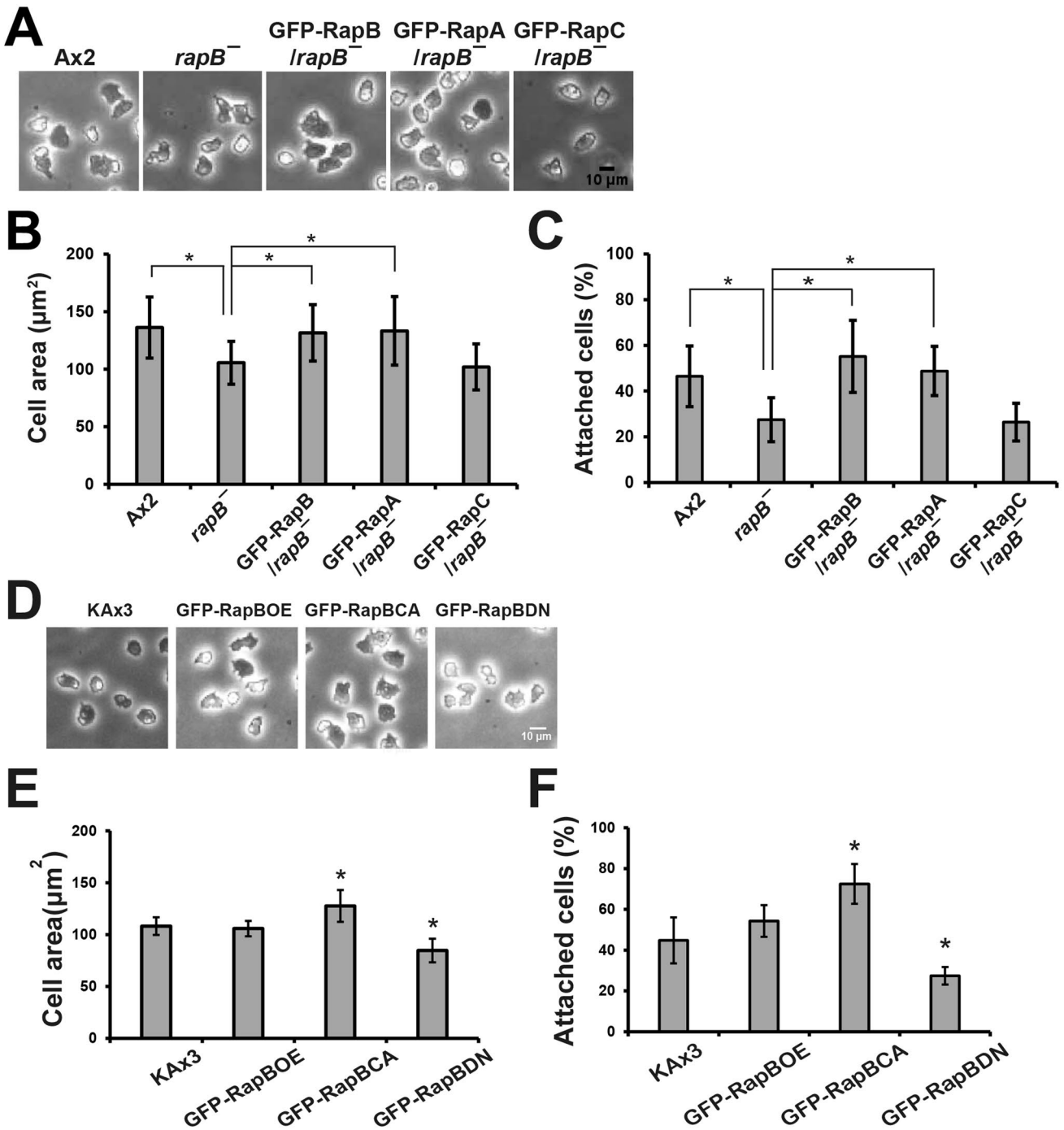

Fig. 2 Cell spreading and adhesion of *rapB* null cells and RapB-overexpressing cells. **A** Cell morphology of wild-type Ax2 cells, *rapB* null cells, and *rapB* null cells expressing GFP-RapB, GFP-RapA, and GFP-RapC. Ax2 wild-type cells were used as the parental strain for *rapB* null cells. **B** Measurement of cell area using Image J software. The values are the means ± SD of three independent experiments. *$p < 0.05$ compared to the control using student's *t*-test. **C** Cell-substrate adhesion. Adhesion of the cells to the substrate was expressed as a percentage of attached cells to total cells. The values are the means ± SD of three independent experiments. *$p < 0.05$ compared to the control. **D** Cell morphology of cells overexpressing RapB. Wild-type RapB was mutated to the constitutively active or the dominantly negative form of RapB and GFP-fused RapB were introduced into wild-type KAx3 cells; GFP-RapBOE, expressing wild-type form of RapB; GFP-RapBCA, expressing the constitutively active form of RapB; GFP-RapBDN, expressing the dominantly negative form of RapB. **E** Measurement of cell area of cells overexpressing RapB. **F** Cell-substrate adhesion of cells overexpressing RapB. The values are the means ± SD of three independent experiments. *$p < 0.05$ compared to the control

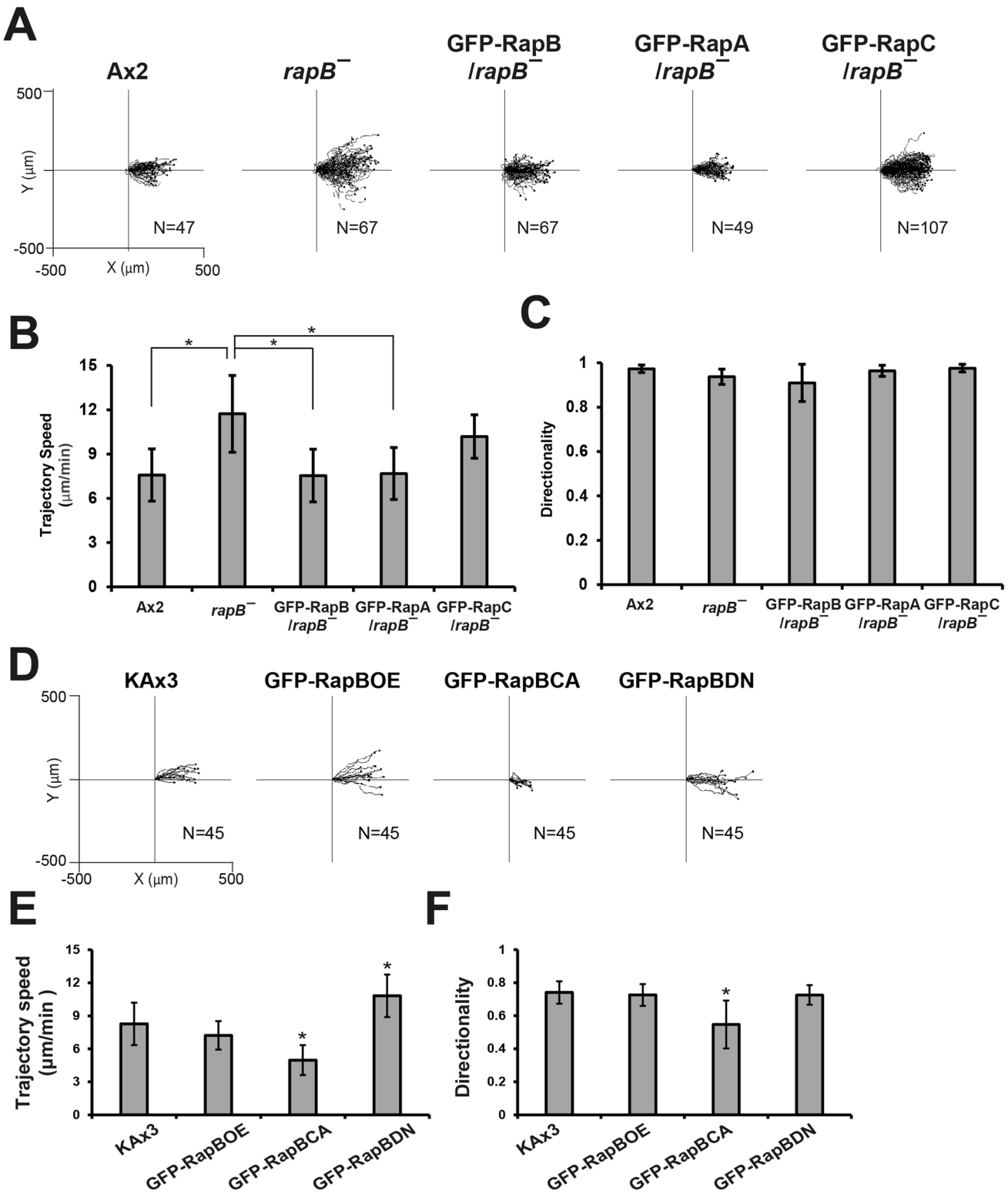

II and total RNAs from wild-type and insertion-mutant cells showed bands of 301 and 445 bp, respectively. When primers I/III, which are specific to the insertion site, were used in RT-PCR, no band was detected in wild-type cells, while a band of 129 bp was observed in the insertion mutant cells (Fig. S1B). These results indicate that the insertion mutant cells have a 144-bp insertion at the site of the gene and transcribe a 144-bp longer transcript than wild-type cells. To

◂**Fig. 3** Chemotaxis of *rapB* null cells and RapB-overexpressing cells. **A** Trajectories of the chemotaxing cells; wild-type Ax2, *rapB* null, and *rapB* null cells expressing GFP-RapB, GFP-RapA, and GFP-RapC. Aggregation-competent cells were prepared by pulsing the cells with cAMP for 5 h and placed in the under-agarose chemotaxis chamber. Movements of the cells up a cAMP chemoattractant gradient were recorded by time-lapse photography for 1 h at 1 min intervals. Plots show migration path of the cells with the start position of each cell centered at point 0. Cells migrate toward the increasing gradients of cAMP on the right. Each line represents the track of a single chemotaxing cell. **B** Quantification of cell motility. The recorded images were analyzed using ImageJ software. Trajectory speed indicates the migration speed of the cells along the total path. **C** Directionality is a measure of how straight the cells move. Cells migrating in a straight line have a directionality of 1. The values are the means ± SD of three independent experiments. Statistically different from control $*p < 0.05$ using the student's *t*-test. **D** Trajectories of the chemotaxing cells; wild-type KAx3 cells and cells expressing GFP-RapBOE, GFP-RapBCA, and GFP-RapBDN during chemotaxis. **E** Quantification of cell motility of RapB-overexpressing cells. Trajectory speed of the chemotaxing cells. **F** Directionality of the cells. The values are the means ± SD of three independent experiments. Statistically different from control $*p < 0.05$ by the student's *t*-test

further examine the function of RapB, we prepared cells overexpressing GFP-fused RapB proteins: a wild-type form (RapBOE), a constitutively active form (RapBCA), and a dominantly negative form (RapBDN). Constitutively active and dominantly negative forms of RapB were prepared by point-mutation of glycine at position 31 to valine (G31V) and serine at position 36 to asparagine (S36N), respectively (Rebstein et al., 1997; Simanshu et al., 2017). Protein expression was confirmed via western blot using an anti-GFP antibody (Fig. S1C).

RapB is Involved in Controlling Cell Morphology and Cell Adhesion

To investigate the function of RapB in controlling cell morphology, we examined cell morphology and size of *rapB* null cells (Fig. 2A). *rapB* null cells were smaller and more rounded than wild-type cells. Measurement of cell areas using ImageJ software showed that *rapB* null cells were approximately two-thirds the size of wild-type cells. These phenotypes were recovered by RapB or RapA expression, but not by RapC expression (Fig. 2A and B). Next, cell adhesion was examined by measuring the fraction of cells attached to the plates during agitation. Compared with wild-type cells, *rapB* null cells showed decreased cell adhesion (Fig. 2C). *rapB* null cells expressing GFP-RapB or GFP-RapA exhibited slightly increased cell adhesion compared to wild-type cells. When GFP-RapC was introduced and expressed in *rapB* null cells, the decrease in cell adhesion was not reversed. These results suggest that RapB is required for cell spreading and cell-substrate adhesion, similar to RapA. Consistent with these results, cells expressing GFP-RapBCA were flattened and highly adhesive, whereas GFP-RapBDN cells were loosely attached to the bottom compared to wild-type cells (Fig. 2E and F). These results suggest that activated RapB induces cell spreading and increases cell adhesion.

RapB Plays an Inhibitory Role in the Control of Migration Speed During Chemotaxis

RapA plays an important role in cell migration via cytoskeletal reorganization during chemotaxis (Jeon et al., 2007a, 2007b; Lee & Jeon, 2012). We expected RapB, which has high homology with RapA, to play an important role in cell migration, and performed cAMP-directed cell migration experiments (Fig. 3). Aggregation-competent cells were prepared by pulsing with 7.5 μM cAMP in Na/K phosphate buffer for 6 h. When the cells were exposed to the chemoattractant gradients, wild-type cells moved towards chemoattractants with an average speed of approximately 7.5 μm/min and directionality of 0.97, which is a measure of how straight the cells move toward the chemoattractant. *rapB* null cells were more polarized and elongated than wild-type cells. *rapB* null cells moved toward increasing cAMP concentrations with higher migration speeds of 11.7 μm/min than wild-type cells and 0.93 directionality similar to wild-type cells. The increased migration speed in *rapB* null cells decreased to the level observed in wild-type cells when GFP-RapB or GFP-RapA was introduced into *rapB* null cells. GFP-RapC was unable to rescue the increased migration rate of *rapB* null cells. The directionality of the cells was indistinguishable among the cells (Fig. 3). These results suggest that RapB plays an inhibitory role in controlling migration speed. The inhibitory effect of RapB on cell migration was similar to that of RapA. Taken together with the cell adhesion results, RapB is likely to control migration speed by regulating cell adhesion.

In support of these results, RapBCA cells showed a markedly decreased migration speed, while RapBDN cells displayed an increased migration speed (Fig. 3D and E). The directionality of RapBOE and RapBDN cells was similar to that of wild-type cells, but RapBCA cells showed decreased directionality during migration, which might be due to the highly spread cell morphology and low migration speed (Fig. 3F). These results support the inhibitory function of RapB on cell migration and suggest that the activated form of RapB is more effective in the controlling cell migration.

Upon starvation, *Dictyostelium* cells release cAMP, causing the surrounding cells to migrate toward the cAMP source and initiate their molecular development to form a multicellular fruiting body (Chisholm & Firtel, 2004). As *rapB* null cells were highly motile and had a higher migration speed during chemotaxis than wild-type cells, we investigated the possible roles of RapB in development (Fig. 4). All cells, including wild-type, *rapB* null, *rapB* null cells expressing

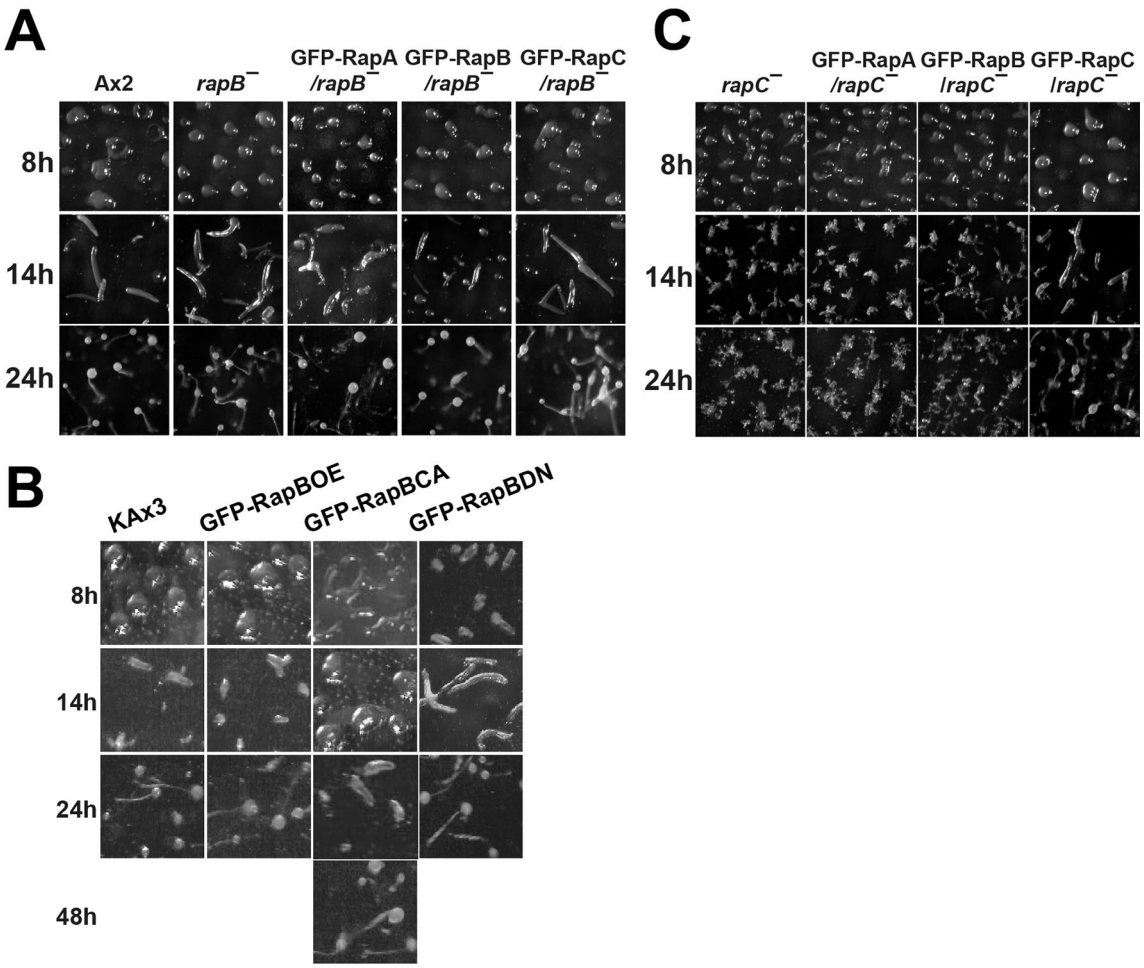

Fig. 4 Multicellular development of the cells. **A** Development of wild-type Ax2, *rapB* null cells, and *rapB* null cells expressing GFP-RapA, GFP-RapB, and GFP-RapC. Exponentially growing cells were washed and developed on non-nutrient agar plates. Photographs were taken at the indicated times after plating. Representative developmental images at the developmental stages were presented. **B** Development of wild-type KAx3 and RapB-overexpressing cells. **C** Development of *rapC* null cells and *rapC* null cells expressing GFP-RapA, GFP-RapB, and GFP-RapC

GFP-RapB, GFP-RapA, and GFP-RapC, exhibited a normal developmental process, with the aggregation stage occurring within 8 h, the slug stage within 14 h, and the formation of fruiting bodies within 24 h (Fig. 4A). However, GFP-RapBCA cells showed slightly delayed aggregation and formation of fruiting bodies compared to wild-type cells (Fig. 4B). Similar developmental phenotypes were observed in cells expressing RapA or RapACA cells (Jeon et al., 2007b). In contrast to RapA and RapB, RapC is involved in the developmental process and the regulation of the tip-forming stage (Park et al., 2018). Cells lacking RapC formed multitipped aggregates. The phenotypes of *rapC* null cells with multiple tips during development were not rescued by the expression of GFP-RapA or GFP-RapB (Fig. 4C). These results indicate that RapB is unlikely to be involved in multicellular developmental processes, unlike RapC that has a unique function in controlling the tip formation stage during development.

RapA and RapB are Unable to Complement the Phenotypes of Cells Lacking RapC

RapB functions similar to RapA in regulating cell morphology, adhesion, and migration in the previous results. RapC has been reported to have a function opposite to that of RapA in cell adhesion and migration (Jeon et al., 2021; Kim et al., 2021). To determine the compatibility of RapB with RapC in controlling cell morphology, cell adhesion, and migration, we examined whether RapB could rescue the phenotypes of *rapC* null cells (Fig. 5). *rapC* null cells show diverse phenotypes, including a highly spread morphology, increased cell adhesion, and decreased migration speed during chemotaxis. These phenotypes of *rapC* null cells were complemented

by the expression of GFP-RapC, but not by GFP-RapA or GFP-RapB (Fig. 5). Cells lacking RapC flattened more than wild-type cells and had approximately 1.7-fold larger areas (Fig. 5A and B). While wild-type cells showed approximately 50% attachment to the substrate after agitation of the plates and removal of the unattached cells, almost all *rapC* null cells remained on the plates (Fig. 5C). During chemotaxis, *rapC* null cells showed decreased migration speed (Fig. 5D and E) and normal directionality (Fig. 5F). Similar to previous experiments, the decreased migration speed of *rapC* null cells was complemented by expressing GFP-RapC but not GFP-RapA or GFP-RapB. These results support previous findings that RapC has a function opposite to that of RapA and RapB in regulating cell morphology and cell adhesion.

Discussion

The present study investigated the role of an uncharacterized RapB protein in *Dictyostelium*, focusing on cell adhesion, migration, and developmental processes, and aimed to understand the functional relationships among RapA, RapB, and RapC. The results demonstrate that RapB is another key player in regulating cell morphology, adhesion, and migration, similar to RapA.

Generation of *rapB* null cells using the CRISPR/Cas9 system allowed an in-depth examination of the phenotypic consequences associated with the absence of RapB. Additionally, we explored the relationship among RapA, RapB, and RapC by analyzing the phenotypes of *rapB* null cells expressing either RapA or RapC. *rapB* null cells exhibit altered cell size, reduced cell-substrate adhesion, and increased migration speed during chemotaxis. Rescue experiments with GFP-fused Rap revealed that RapB and RapA, but not RapC, restored normal cell morphology and adhesion, indicating functional similarities between RapA and RapB. Furthermore, this study sheds light on the inhibitory role of RapB in controlling the migration speed during chemotaxis, paralleling the functions of RapA. The activation states of RapB, illustrated by the GFP-RapB mutants (constitutively active and dominantly negative forms), further support its involvement in the regulation of cell migration.

This study provides insights into the developmental aspects of RapB. Despite the altered migration phenotype of *rapB* null cells, the multicellular developmental process remained unaffected, distinguishing RapB from RapC, which plays a unique role in tip formation during development (Park et al., 2018). Investigation into the complementation of *rapC* null cell phenotypes by Rap proteins revealed that RapB, similar to RapA, was unable to rescue the spread morphology, increased cell adhesion, and decreased migration speed observed in *rapC* null cells. These findings support the notion that RapB and RapC have opposing functions in regulating cell morphology and adhesion.

Investigating the role of *Dictyostelium* RapB in cell adhesion and migration has significant implications for our understanding of Ras subfamily proteins, particularly Rap proteins, and their evolutionarily conserved functions across species. The findings from this study are consistent with mammalian Rap proteins, specifically Rap1 and Rap2, shedding light on the potential conserved mechanisms of cell regulation. Moreover, the inability of RapB to complement the phenotypes of *rapC* null cells in *Dictyostelium* finds a counterpart in the mammalian system. Mammalian Rap1 and Rap2, despite their structural similarities, often exhibit distinct functions in various cellular processes. Conflicting effects on endothelial barrier resistance have been documented for mammalian Rap1 and Rap2 (Pannekoek et al., 2013). Activation of Rap1 enhances barrier resistance, whereas activation of Rap2 diminishes this effect, exerting opposing effects on the control of endothelial barrier resistance. Rap1 and Rap2 share similar guanine nucleotide exchange factors (GEFs), GTPase-activating proteins (GAPs), and downstream effector proteins (Bos, 2018; Nussinov et al., 2020). However, the precise mechanism by which Rap1 and Rap2 function antagonistically during cell adhesion and migration remains unclear. One plausible explanation is that Rap1 and Rap2 may compete for the same set of GEFs, GAPs, and effector proteins, with Rap2 acting as a counteractive molecular switch in the Rap1 signaling cascade. Similar to RapA, RapB failed to rescue the phenotypes of *rapC* null cells, which aligns with the functional divergence observed between Rap1 and Rap2 in mammals. This raises intriguing questions regarding the evolutionary and functional relationships among Rap proteins in different organisms.

In conclusion, our study elucidates the previously uncharacterized role of RapB in *Dictyostelium*, revealing its involvement in cell adhesion and migration and its inability to complement the functions of RapC. These findings contribute to our understanding of the intricate regulatory network involving Rap proteins in cellular processes and open avenues for future investigations into the underlying mechanisms.

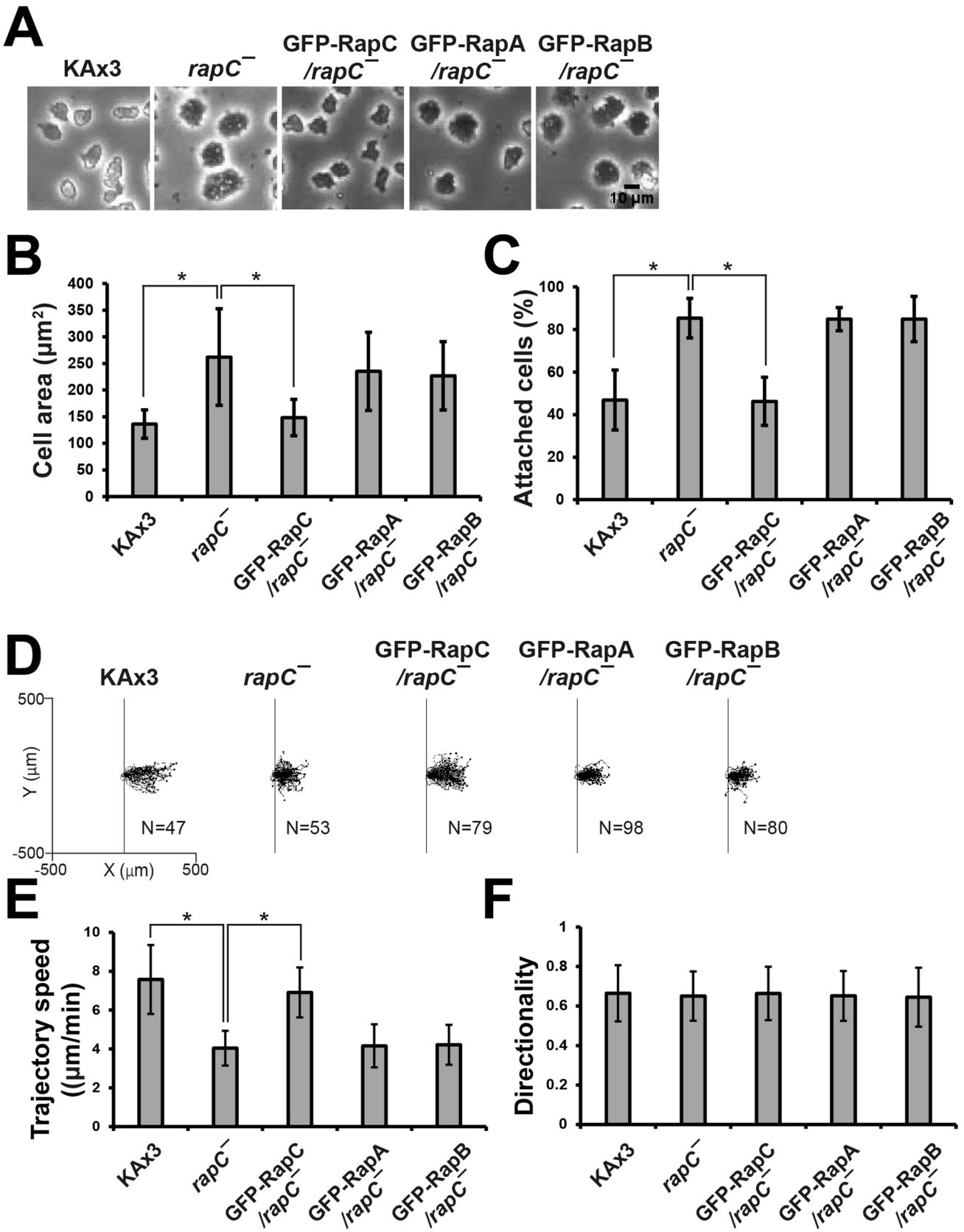
A
KAx3
rapC¯
GFP-RapC /rapC¯
GFP-RapA /rapC¯
GFP-RapB /rapC¯
10 μm
B
Cell area (μm²)
400
350
300
250
200
150
100
50
0
*
*
KAx3
rapC¯
GFP-RapC /rapC¯
GFP-RapA /rapC¯
GFP-RapB /rapC¯
C
Attached cells (%)
100
80
60
40
20
0
*
*
KAx3
rapC¯
GFP-RapC /rapC¯
GFP-RapA /rapC¯
GFP-RapB /rapC¯
D
KAx3
rapC¯
GFP-RapC /rapC¯
GFP-RapA /rapC¯
GFP-RapB /rapC¯
500
Y (μm)
-500
-500
X (μm)
500
N=47
N=53
N=79
N=98
N=80
E
Trajectory speed ((μm/min)
10
8
6
4
2
0
*
*
KAx3
rapC¯
GFP-RapC /rapC¯
GFP-RapA /rapC¯
GFP-RapB /rapC¯
F
Directionality
1
0.8
0.6
0.4
0.2
0
KAx3
rapC¯
GFP-RapC /rapC¯
GFP-RapA /rapC¯
GFP-RapB /rapC¯

◂**Fig. 5** Complementation of the phenotypes of *rapC* null cells with Rap proteins. **A** Cell morphology of wild-type KAx3, *rapC* null cells, and *rapC* null cells expressing GFP-RapA, GFP-RapB, and GFP-RapC. KAx3 wild-type cells were used as the parental strain for *rapC* null cells. *rapC* null cells were introduced with GFP-RapA, GFP-RapB, and GFP-RapC. The phenotypes of *rapC* null cells in cell morphology were compared to those of wild-type KAx3 cells and *rapC* null cells expressing GFP-RapA, GFP-RapB, and GFP-RapC. **B** Quantification of cell areas. **C** Cell-substrate adhesion. The values are the means ± SD of three independent experiments. $*p < 0.05$ compared to the control by student's *t*-test. **D** Trajectories of the chemotaxing cells, *rapC* null cells and *rapC* null cells expressing GFP-RapA, GFP-RapB, and GFP-RapC. Quantification of trajectories (**E**) and directionalities (**F**) of the chemotaxing cells. The values are the means ± SD of three independent experiments. Statistically different from control $*p < 0.05$ using the student's *t*-test

Supplementary Information The online version contains supplementary material available at https://doi.org/10.1007/s12275-024-00143-y.

Acknowledgements This work was supported by the National Research Foundation of Korea (NRF) grant funded by the Korea government (MSIT) (2021R1F1A1047695) and the research fund from Chosun University to T. J. Jeon (2023).

Declarations

Conflict of Interest The authors declare no conflict of interest.

References

Artemenko, Y., Lampert, T. J., & Devreotes, P. N. (2014). Moving towards a paradigm: Common mechanisms of chemotactic signaling in *Dictyostelium* and mammalian leukocytes. *Cellular and Molecular Life Sciences, 71*, 3711–3747.

Bos, J. L. (2018). From Ras to Rap and back, a journey of 35 years. *Cold Spring Harbor Perspectives in Medicine, 8*, a031468.

Chisholm, R. L., & Firtel, R. A. (2004). Insights into morphogenesis from a simple developmental system. *Nature Reviews Molecular Cell Biology, 5*, 531–541.

Jeon, J., Kim, D., & Jeon, T. J. (2021). Opposite functions of RapA and RapC in cell adhesion and migration in *Dictyostelium*. *Animal Cells and Systems, 25*, 203–210.

Jeon, T. J., Lee, D. J., Lee, S., Weeks, G., & Firtel, R. A. (2007a). Regulation of Rap1 activity by RapGAP1 controls cell adhesion at the front of chemotaxing cells. *The Journal of Cell Biology, 179*, 833–843.

Jeon, T. J., Lee, D. J., Merlot, S., Weeks, G., & Firtel, R. A. (2007b). Rap1 controls cell adhesion and cell motility through the regulation of myosin II. *The Journal of Cell Biology, 176*, 1021–1033.

Jeon, T. J., Lee, S., Weeks, G., & Firtel, R. A. (2009). Regulation of *Dictyostelium* morphogenesis by RapGAP3. *Developmental Biology, 328*, 210–220.

Kim, D., Kim, W., & Jeon, T. J. (2021). Reversible function of RapA with the C-terminus of RapC in *Dictyostelium*. *Journal of Microbiology, 59*, 848–853.

Kölsch, V., Charest, P. G., & Firtel, R. A. (2008). The regulation of cell motility and chemotaxis by phospholipid signaling. *Journal of Cell Science, 121*, 551–559.

Kortholt, A., & van Haastert, P. J. (2008). Highlighting the role of Ras and Rap during *Dictyostelium* chemotaxis. *Cellular Signalling, 20*, 1415–1422.

Lee, M. R., & Jeon, T. J. (2012). Cell migration: Regulation of cytoskeleton by Rap1 in *Dictyostelium discoideum*. *Journal of Microbiology, 50*, 555–561.

Mun, H., & Jeon, T. J. (2012). Regulation of actin cytoskeleton by Rap1 binding to RacGEF1. *Molecules and Cells, 34*, 71–76.

Mun, H., Lee, M. R., & Jeon, T. J. (2014). RapGAP9 regulation of the morphogenesis and development in Dictyostelium. *Biochemical and Biophysical Research Communications, 446*, 428–433.

Muramoto, T., Iriki, H., Watanabe, J., & Kawata, T. (2019). Recent advances in CRISPR/Cas9-mediated genome editing in *Dictyostelium*. *Cells, 8*, 46.

Nussinov, R., Jang, H., Zhang, M., Tsai, C. J., & Sablina, A. A. (2020). The mystery of Rap1 suppression of oncogenic Ras. *Trends in Cancer, 6*, 369–379.

Pannekoek, W. J., Linnemann, J. R., Brouwer, P. M., Bos, J. L., & Rehmann, H. (2013). Rap1 and Rap2 antagonistically control endothelial barrier resistance. *PLoS One, 8*, e57903.

Park, B., Kim, H., & Jeon, T. J. (2018). Loss of RapC causes defects in cytokinesis, cell migration, and multicellular development of *Dictyostelium*. *Biochemical and Biophysical Research Communications, 499*, 783–789.

Rebstein, P. J., Cardelli, J., Weeks, G., & Spiegelman, G. B. (1997). Mutational analysis of the role of Rap1 in regulating cytoskeletal function in *Dictyostelium*. *Experimental Cell Research, 231*, 276–283.

Sasaki, A. T., Janetopoulos, C., Lee, S., Charest, P. G., Takeda, K., Sundheimer, L. W., Meili, R., Devreotes, P. N., & Firtel, R. A. (2007). G protein-independent Ras/PI3K/F-actin circuit regulates basic cell motility. *The Journal of Cell Biology, 178*, 185–191.

Sekine, R., Kawata, T., & Muramoto, T. (2018). CRISPR/Cas9 mediated targeting of multiple genes in *Dictyostelium*. *Scientific Reports, 8*, 8471.

Simanshu, D. K., Nissley, D. V., & McCormick, F. (2017). RAS proteins and their regulators in human disease. *Cell, 170*, 17–33.

Wennerberg, K., Rossman, K. L., & Der, C. J. (2005). The Ras superfamily at a glance. *Journal of Cell Science, 118*, 843–846.

Zhou, Y., & Hancock, J. F. (2015). Ras nanoclusters: Versatile lipid-based signaling platforms. *Biochimica Et Biophysica Acta, 1853*, 841–849.